Supporting Information for: Ion-induced formation of nanocrystalline cellulose colloidal glasses containing nematic domains

Pascal Bertsch,*,† Antoni Sánchez-Ferrer,† Massimo Bagnani,† Stéphane Isabettini,† Joachim Kohlbrecher,‡ Raffaele Mezzenga,† and Peter Fischer*,†

†*Institute of Food Nutrition and Health, ETH Zurich, 8092 Zurich, Switzerland*

‡*Laboratory for Neutron Scattering and Imaging, Paul Scherrer Institute, 5232 Villigen PSI, Switzerland*

E-mail: pascal.bertsch@hest.ethz.ch; peter.fischer@hest.ethz.ch

Phone: +41 44 632 67 62

Contents (7 pages)

Approximation of the isotropic-cholesteric phase transition

To calculate the critical volume fraction ϕ_c for the isotropic-cholesteric phase transition an adaptation of Onsager's formula was employed that accounts for the effective diameter D_{eff} of charged particles:[1]

$$\phi_c = 3.34\frac{D^2}{D_{eff}L} \tag{1}$$

where D and L are the width and length of NCC, respectively. D_{eff} is given by:

$$D_{eff} = D + k^{-1}(lnA + C + ln2 - \frac{1}{2}) \tag{2}$$

where k^{-1} is the Debye length, C the Euler constant, and A corresponds to:

$$A = 2\pi\upsilon_{eff}^2 k^{-1} Q exp(-kD) \tag{3}$$

where υ_{eff} is the effective linear charge density and Q the Bjerrum length. D = 4.8 nm and L = 78.6 nm were previously determined by atomic force microscopy.[2] The charge density was assessed titrimetrically to 0.33 mmol/g.[3] Assuming all charges on the surface of NCC, this corresponds to υ_{eff} = 0.67 nm^{-1}. The ionic strength of NCC dispersions was approximated to 1.5 mM from its conductivity, resulting in k^{-1} = 7.8 nm. The Bjerrum length Q is 0.7 nm in water at room temperature. This results in D_{eff} = 27.4 nm and ϕ_c = 0.035. Upon addition of 2 mM NaCl, k^{-1} is decreased to 5.1 nm. This decreases the approximated D_{eff} to 15.8 nm, resulting in ϕ_c = 0.061. To determine the critical mass fraction, we assumed 1.5 g/cm^3 as the density of NCC, resulting in 5.1 and 8.8 wt% for 0 and 2 mM added salt, respectively.

Supplementary Figures and Discussion

Figure S1 demonstrates salt-induced phase transitions of NCC dispersions induced with $CaCl_2$ instead of NaCl. The same phases transitions may be induced using $CaCl_2$, although at lower salt concentrations due to more efficient charge screening of divalent salts. Depending on NCC concentration, an attractive glass may already be formed at 1-2 mM, and hydrogels at $>$ 5 mM $CaCl_2$. This can be attributed to the ionic strength induced by divalent salts which is four times higher compared to monovalent salts at the same concentration. A detailed investigation of NCC dispersion phase transitions using NaCl, KCl, $CaCl_2$, and $MgCl_2$ was provided earlier.[3] Similar results were reported by Phan-Xuan et. al,[4] who showed that NCC charge screening is even more efficient with trivalent $FeCl_3$.

Figure S2 shows the structure factors obtained by dividing SAXS intensity profiles by the form factor extracted from the SAXS profile of 0.02 wt% NCC dispersions. The red line corresponds to the square well potential model fit shown in the main manuscript.

Figure S3 provides the SAXS intensity profiles of 2 and 5 wt% NCC dispersions upon NaCl addition for the entire q-range investigated. Additional NaCl concentrations are shown compared to the main manuscript.

Figure S4 depicts small angle neutron scattering (SANS) intensity profiles for 2 and 5 wt% NCC with added $CaCl_2$ instead of NaCl. The SANS profiles of NCC dispersions without salt addition confirmed the appearance of a structure peak at q $\approx$ 0.11 and 0.18 nm^{-1} for 2 and 5 wt% NCC, respectively. Upon addition of $CaCl_2$ the structure peak diminished, in agreement with results from SAXS using NaCl. In our previous study we considered the structure peak proof for the presence of anisotropic nematic domains.[3] This interpretation was probably not correct in-light of the present SAXS data showing a decrease of the structure peak upon salt addition followed by a new peak at q = 0.057 and 0.073 nm^{-1} for 2 and 5 wt% NCC, respectively, more likely associated with nematic domains. This peak was not observed in SANS at the $CaCl_2$ concentrations investigated.

Materials and Methods

Small angle neutron scattering. SANS was conducted at the Swiss Spallation Neutron Source SINQ at Paul Scherrer Institute (Villigen PSI, Switzerland) at the SANS II beamline. Samples were prepared as described in the main manuscript in D_2O with $CaCl_2$ (anhydrous, Amresco, USA) and loaded in 2 mm thick Hellma quartz cuvettes (Müllheim, Germany). A 2D ^{3}He detector was placed 6, 4, and 1.22 m from the sample and the neutron wavelength fixed at 1.08, 0.476, and 0.476 nm, respectively. The empty cuvette and D_2O were recorded for background corrections. Experiments were performed at 18 °C. Radially averaged scattering curves were computed from the 2D scattering patterns using the BerSANS software.

References

(1) Mezzenga, R.; Jung, J. M.; Adamcik, J. Effects of charge double layer and colloidal aggregation on the isotropic-nematic transition of protein fibers in water. *Langmuir* **2010**, *26*, 10401–10405.

(2) Bertsch, P.; Diener, M.; Adamcik, J.; Scheuble, N.; Geue, T.; Mezzenga, R.; Fischer, P. Adsorption and interfacial layer structure of unmodified nanocrystalline cellulose at air/water interfaces. *Langmuir* **2018**, *34*, 15195–15202.

(3) Bertsch, P.; Isabettini, S.; Fischer, P. Ion-induced hydrogel formation and nematic ordering of nanocrystalline cellulose suspensions. *Biomacromolecules* **2017**, *18*, 4060–4066.

(4) Phan-Xuan, T.; Thuresson, A.; Skepö, M.; Labrador, A.; Bordes, R.; Matic, A. Aggregation behavior of aqueous cellulose nanocrystals: the effect of inorganic salts. *Cellulose* **2016**, *23*, 3653–3663.

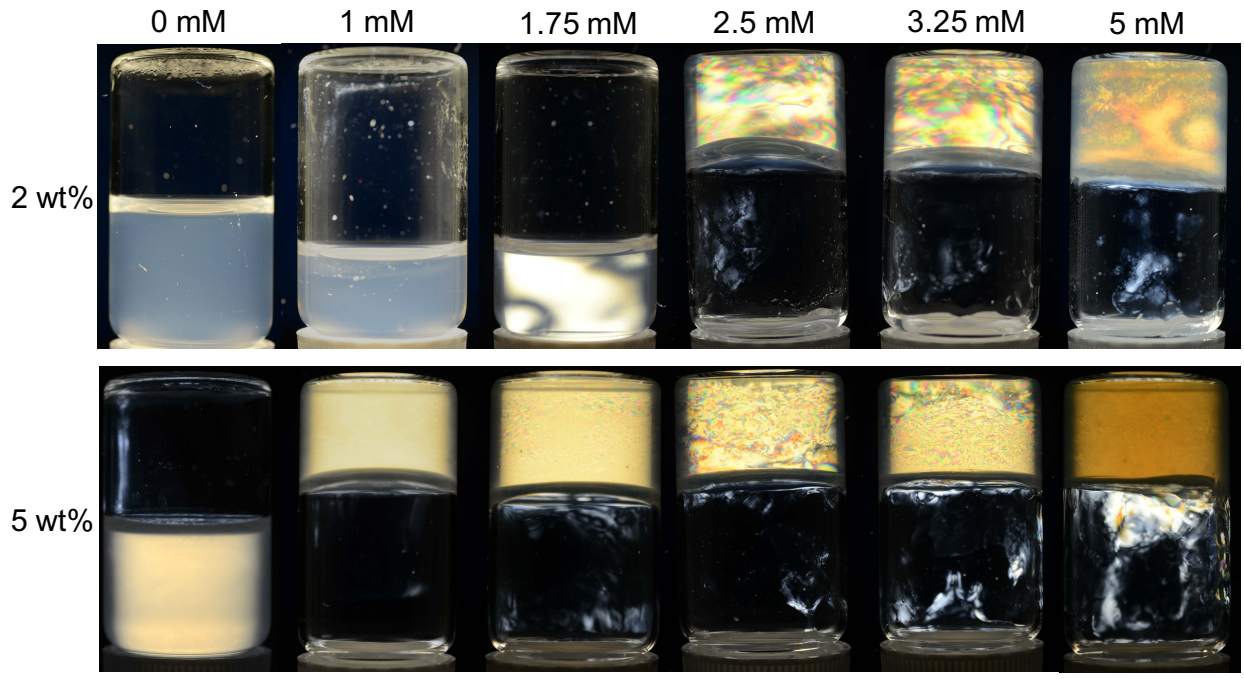

Figure S1: Visualization of salt-induced phase transitions upon addition of $CaCl_2$ to 2 and 5 wt% NCC dispersions placed between cross-polarizers. Samples were prepared in D_2O for SANS experiments.

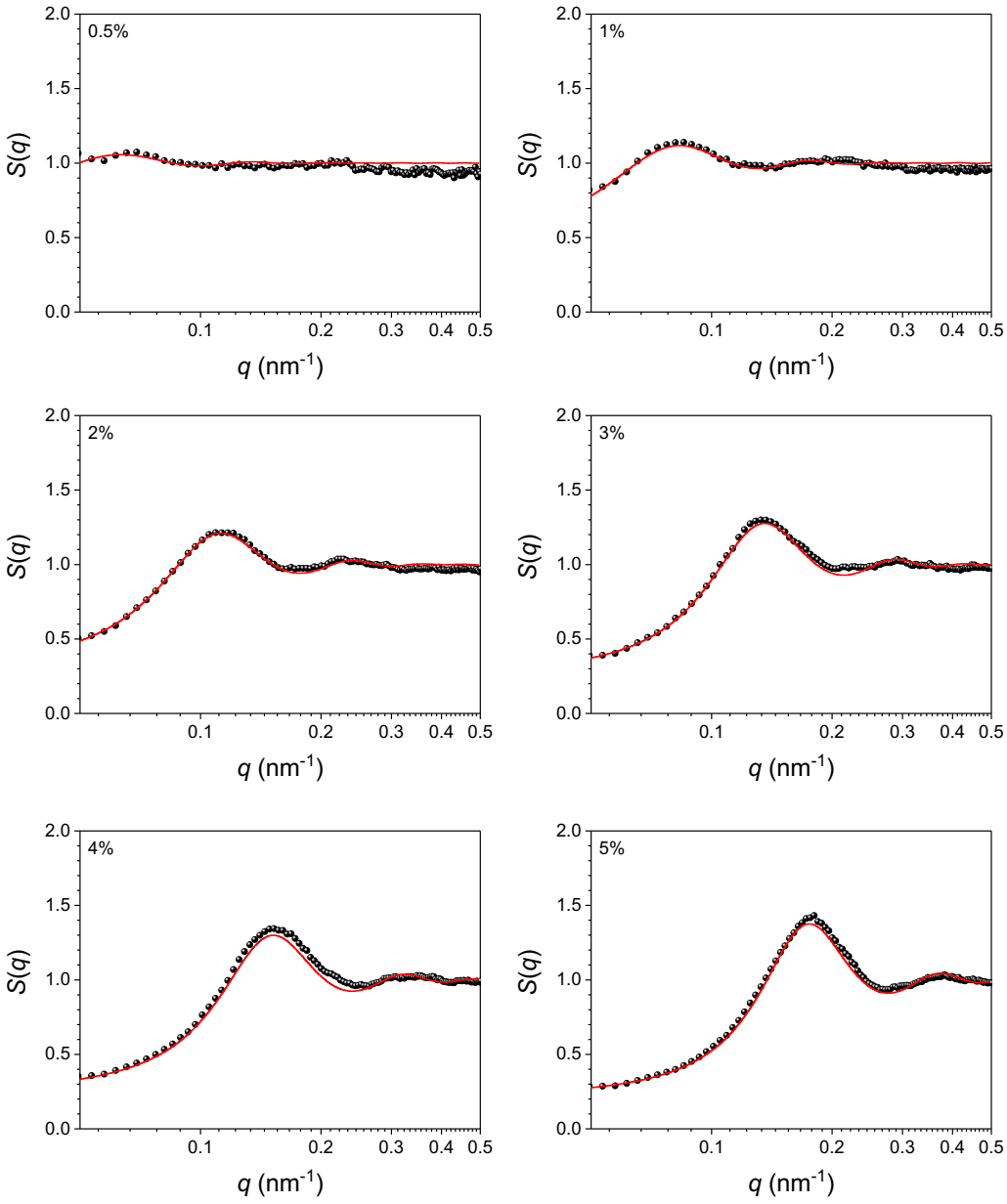

Figure S2: Structure factors of NCC dispersions at different concentrations obtained from SAXS intensity profiles and fitted square well potential model (red line).

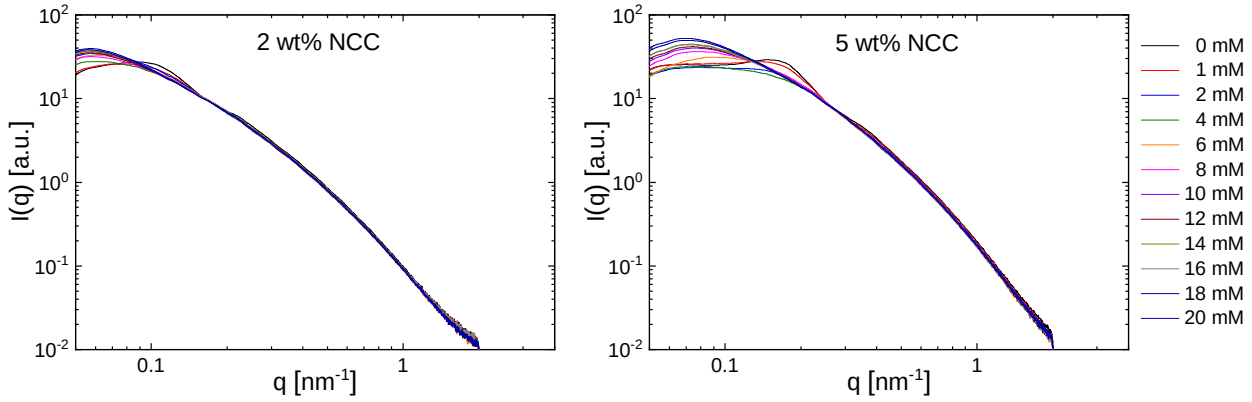

Figure S3: 1D SAXS intensity profiles of 2 wt% (left) and 5 wt% (right) NCC dispersions at increasing NaCl concentration.

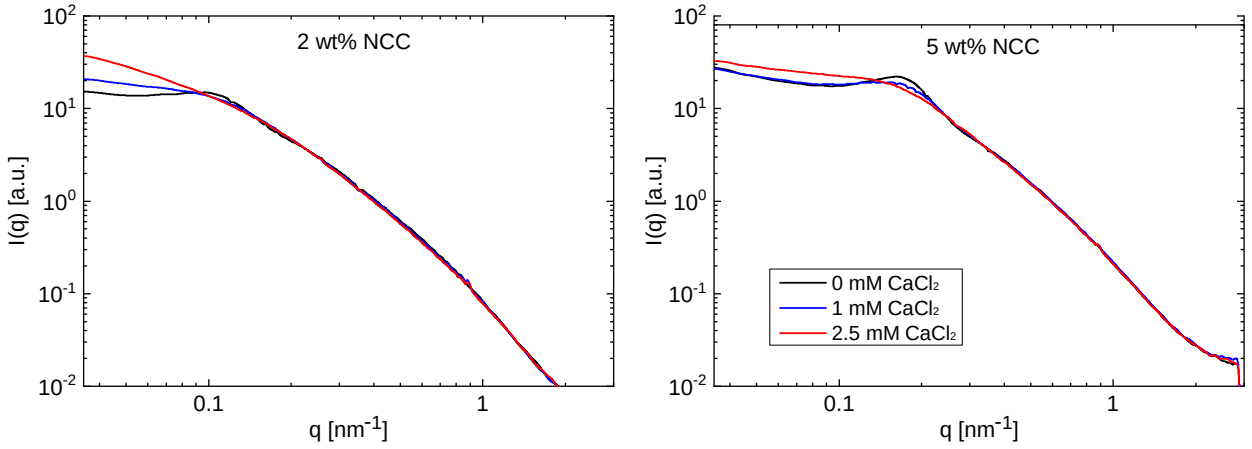

Figure S4: 1D SANS intensity profiles of 2 wt% (left) and 5 wt% (right) NCC dispersions at increasing $CaCl_2$ concentration.